Zeeman Effect Studies of the $^5I_7$–$^5I_8$ Transition in CaF_2:Dy^{2+}

Z. J. KISS, C. H. ANDERSON, AND R. ORBACH*
RCA Laboratories, Princeton, New Jersey
(Received 5 October 1964)

Zeeman effect studies of $^5I_7$–$^5I_8$ fluorescent transitions of the CaF_2:Dy^{2+} system were carried out. The symmetries and the spectroscopic splitting factors of a number of crystal field components were determined, and the transitions were found to be of magnetic dipole origin. Effects due to magnetic interactions among the lowest three crystal field components of the ground state were observed. The orientation dependence of the Zeeman pattern of the $|7T_1^{(2)}\rangle \rightarrow |8T_2^{(2)}\rangle$ laser transition is treated.

I. INTRODUCTION

SPECTROSCOPIC investigations of divalent rare earth in CaF_2[1,2] revealed that the divalent rare earth sits in a substitutional Ca site in a cubic environment. Consequently, the $4f$ states of the rare earth have no other parity configurations admixed by the static crystal field and the $4f$–$4f$ electric dipole transitions are forbidden, Sharp line transitions in the CaF_2:Tm^{2+} system were found to be of magnetic dipole origin.[3] This paper accompanying the previous article[4] describes Zeeman effect studies of the $^5I_7 \rightarrow {}^5I_8$ transition in the CaF_2:Dy^{2+} system. The purpose of this investigation was to determine the symmetry of the various crystal field states from which the transitions arise, to deduce the magnetic splitting factor for these states, and to obtain the character of the transitions. This work was of further interest, since the CaF_2:Dy^{2+} laser proved to be one of the best existing solid-state lasers; Zeeman tuning of the laser frequency was demonstrated previously.[5,6]

The first part of this paper describes the experimental techniques and the fluorescence spectra. Then the Zeeman studies of the six lines will be discussed. The orientation dependence of the Zeeman components of the laser line will be treated, and finally the nonlinear magnetic interaction among the three lowest levels of the ground state will be considered.

II. EXPERIMENTAL PROCEDURE

Since the oscillator strength of the $4f$–$4f$ transitions of the divalent rare earth in cubic hosts is small, these transitions cannot be readily studied in absorption. On the other hand, the sharp fluorescent transitions coupled with fairly high g values of the rare earths make them especially suitable for Zeeman effect studies, since resonably small magnetic fields ($\sim$10 kG) are sufficient to observe the effect. The fluorescence spectra were studied with a Jarrell-Ash $f/35$ grating spectrometer equipped with a cooled PbS detector. The detector was scanned in the image plane of the spectrometer with a precision micrometer and the signal was recorded using a Perkin-Elmer lock-in amplifier recorder system. The resolution of the spectrometer at 2.4 μ was $\sim$0.25 cm^{-1}, which was also the linewidth of the fluorescent transitions at 78°K.

A 6-in. Varian magnet was used with a tapered 4-in. pole piece and a $1\frac{1}{4}$-in. gap. The maximum field obtainable with the magnet was 14 kG. Crystals were immersed in liquid N_2 temperature and were illuminated with a 600-W tungsten lamp using a water filter. Both transverse and longitudinal Zeeman patterns were taken. For the longitudinal patterns a mirror at 45° to the field direction was inserted to bring out the fluorescent beam. The clearly observable [111] cleavage planes of the CaF_2 were used to orient the crystals.

The fluorescence spectrum of CaF_2:Dy^{2+} consists of a large number of lines in the 2.2 $\mu \rightarrow$ 2.7 μ region of the spectrum.[4] Of these lines there are six that are particularly sharp and prominent at liquid N_2 temperature. The six lines between 2.3 and 2.4 μ are reproduced in Fig. 1. The strongest of these lines line A at 4239.5 cm^{-1} is the laser line, corresponding to the $|7T_1^{(2)}\rangle \rightarrow |8T_2^{(2)}\rangle$ transition. At 4.2°K, only lines A and B remain indicating that the $^5I_7$ state is thermalized. Zeeman effect studies were carried out on all six lines from A to F at liquid N_2 temperature and on lines A and B at 27°K.

III. THE ZEEMAN PATTERN

The Zeeman splitting of line A and the corresponding energy levels are shown on Fig. 2. The pattern arises from two triply degenerate states with nearly identical g values (Table I). The calculated intensity distribution for the various Zeeman patterns assuming magnetic dipole transitions are also shown on Fig. 2. The agreement for a magnetic pattern is excellent. In some cases a discrepancy was found between the observed and predicted pattern, but this was due entirely to the polarization properties of the grating and could be corrected for. The asymmetry of the observed pattern is due to the nonlinear magnetic interaction. From the pattern it can be concluded that the sign of the splitting factors for the two states are different. However, to assign the negative value uniquely to the $|8T_2^{(2)}\rangle$ state (Table I) also required knowledge of the wave

* Present address: Department of Physics, University of California, Los Angeles 24, California.
[1] W. Hayes and J. W. Twidell, J. Chem. Phys. **35**, 1521 (1961).
[2] D. S. McClure and Z. J. Kiss, J. Chem. Phys. **39**, 3251 (1963).
[3] Z. J. Kiss, Phys. Rev. **127**, 718 (1962).
[4] Z. J. Kiss, Phys. Rev. **127**, 718 (1962).
[5] Z. J. Kiss and R. C. Duncan, Proc. IEEE **50**, 1532 (1962).
[6] Z. J. Kiss, Appl. Phys. Letters **3**, 145 (1963).

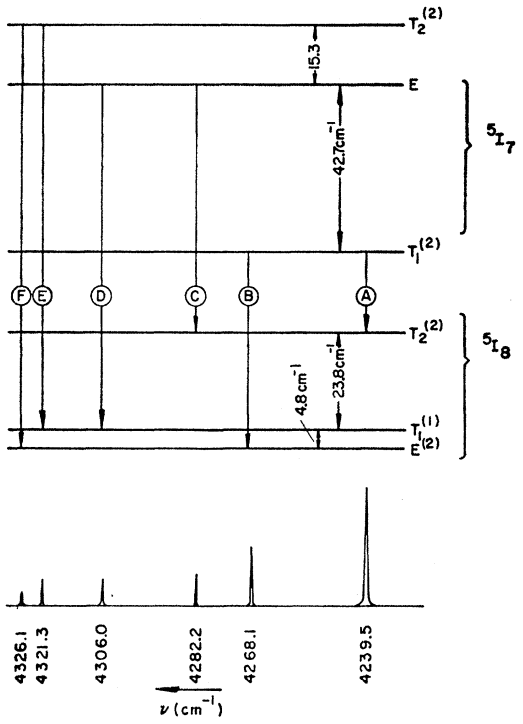

FIG. 1. Energy levels and the fluorescence pattern of some of the prominent $^5I_7 \rightarrow {}^5I_8$ transitions of the CaF_2:Dy^{2+} system.

functions as given in the previous paper.[4] The crystalline quantum number designations "μ" for the T_1 and T_2 state are taken as components of the $l=1$ and $l=2$ orbital wave functions, respectively. In the case of $H\|[100]$ a selection rule $\Delta\mu=0, \pm1$ is observed, which is identical with the magnetic dipole selection rule of $\Delta M=0, \pm1$.[7] The crystalline quantum numbers also describe correctly the polarizations of the transitions. This simple situation only holds for the case when the magnetic field is along one of the high symmetry axes (i.e., $H\|[100]$ or $[111]$), but the general case will be discussed later.

The next strongest line of Fig. 1 is B, corresponding to the $|7T_1^{(2)}\rangle \rightarrow |8E^{(2)}\rangle$ transition. It can be noted on the energy level diagram that a line corresponding to the $|7T_1^{(2)}\rangle \rightarrow |8T_1^{(2)}\rangle$ transition is missing. This line is allowed by magnetic dipole symmetry selection rules, but by an accidental cancellation among components making up the transition probability, its value is down by a factor of 20 000 compared to line A (see Table III of Ref. 4). In the presence of a magnetic field, however, there is strong mixing between the $|8T_1^{(1)}\rangle$ and $|8E^{(2)}\rangle$ states and the $|7T_1^{(2)}\rangle \rightarrow |8T_1^{(1)}\rangle$ transition becomes observable by borrowing intensity from line B. The Zeeman pattern of line B is shown on Fig. 3. Since the $|8E^{(2)}\rangle$ state is a nonmagnetic doublet, in the first

[7] This is strictly true only when it is realized that the magnetic sublevel $\mu=2$ of the $|8T_2^2\rangle$ state has $\mu=\pm2$ character in it as is discussed in Sec. IV.

TABLE I. Magnetic splitting factors for the CaF_2:Dy^{2+} system.

J	State	M	Linear g value Observed	Linear g value Calculated	Nonlinear coefficient B for H:[100] Observed	Nonlinear coefficient B for H:[100] Calculated
7	$T_2^{(2)}$	1			0	
		2	-3.1 ± 0.1	-3.27	$+1.3\pm0.2$	$+1.91$
		-1			0	
7	E	0	0	0	-0.4	-0.44
		2			-2.0 ± 0.2	-1.91
7	$T_1^{(2)}$	1			0	
		0	$+4.73\pm0.05$	$+4.66$	-0.4 ± 0.2	-0.44
		-1			0	
8	$T_2^{(2)}$	1			$+0.3$	$+0.29$
		2	-4.95 ± 0.05	-5.00	$+1.0\pm0.2$	$+1.11$
		-1			$+0.6$	$+0.29$
8	$T_1^{(1)}$	1				-0.29
		0	-4.9 ± 0.1	-4.89	$+6.1\pm0.2$	$+6.8$
		-1				-0.29
8	$E^{(2)}$	2			-1.0	-1.11
		0	0	0	-6.1 ± 0.2	-6.8

$\Delta E=g\beta H+B\beta^2H^2$,
$\beta=0.0467$ cm^{-1}/kG.

approximation only three Zeeman components should be observed. However, again due to the magnetic interaction with the $|8T_1^{(1)}\rangle$ state, the nonmagnetic ground state is split quadratically with magnetic field, and a six line pattern is observed. In this six-line pattern, the unshifted line corresponding to $\Delta\mu=2$ transition is forbidden even in the presence of second-order magnetic interactions, as long as H is exactly $\|[100]$. With a

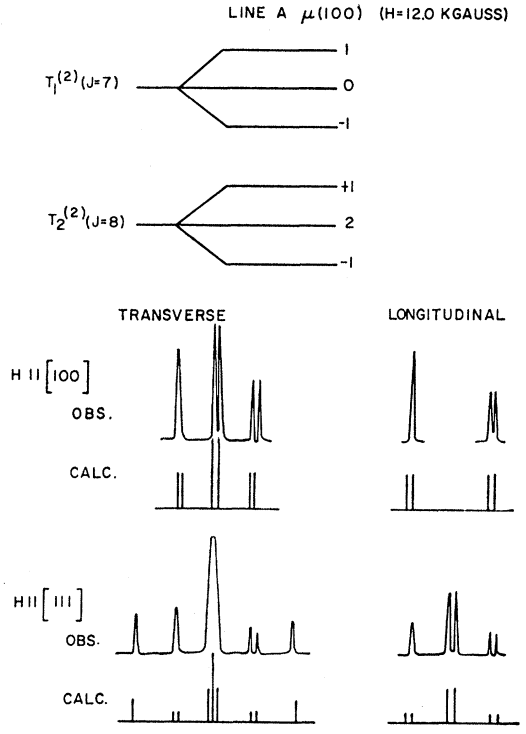

FIG. 2. Observed and calculated Zeeman pattern of the $|7T_1^{(2)}\rangle \rightarrow |8T_2^{(2)}\rangle$ transition.

slight misorientation, the $\mu=\pm1$ character can be admixed into the $\mu=2$ component of the $|8E^{(2)}\rangle$ state and the line may appear. From lines E and F, it can be seen directly that the separation of the $|8E^{(2)}\rangle$ and the next state above it is 4.9 cm^{-1}. The intensity pattern of line B confirms that this next excited state has the symmetry T_1 (and not T_2 as it could possibly be from Fig. 7 of Ref. 4) since the $\mu=0$ component interacts most strongly with the excited state above (for $H\|[100]$). The nonlinear interaction will be discussed later in detail, but it can be noted here that the nonmagnetic ground state in a high field splits, and for H not $\|[100]$, transitions between the two components should be observable in paramagnetic resonance. The paramagnetic resonance studies of Sabisky[8] have indeed confirmed this suggestion.

Line C corresponds to a transition from the next excited state of the $^5I_7$ term which again is a nonmagnetic doublet $|7E\rangle$ (Fig. 4). The pattern again consists of more than three lines since the transition is $|7E\rangle \rightarrow |8T_2^{(2)}\rangle$. Unlike the pattern of B, there are only five lines observed and the forbidden $\Delta\mu=2$ transition is missing. The reason for this is the larger separation of the $|7T_2^{(2)}\rangle$ perturbing level from the doublet $|7E\rangle$ state (15.3 cm^{-1}, see Fig. 1) and with the smaller perturbation the misalignment of H with respect to the crystal axes is not so serious. Again the intensity pattern confirms the assignment of the $|7T_2^{(2)}\rangle$ state above the doublet. The g value of the $|8T_2^{(2)}\rangle$ state determined from the Zeeman pattern of C agrees exactly with the g value determined from the pattern of

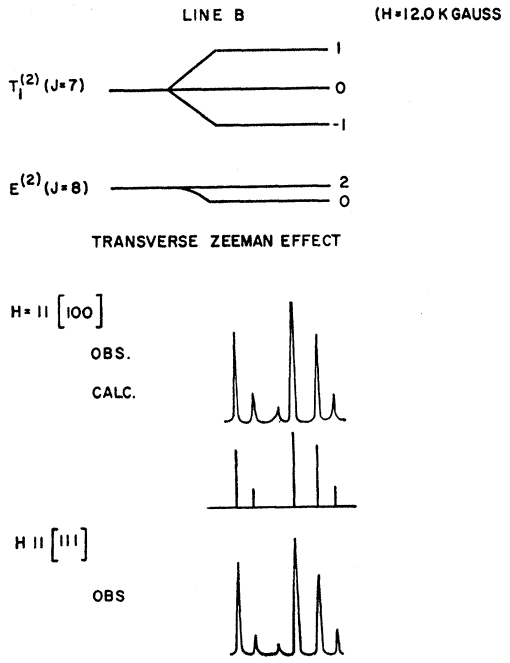

FIG. 3. Observed and calculated Zeeman pattern of the $|7T_1^{(2)}\rangle \rightarrow |8E^{(2)}\rangle$ transition (line B).

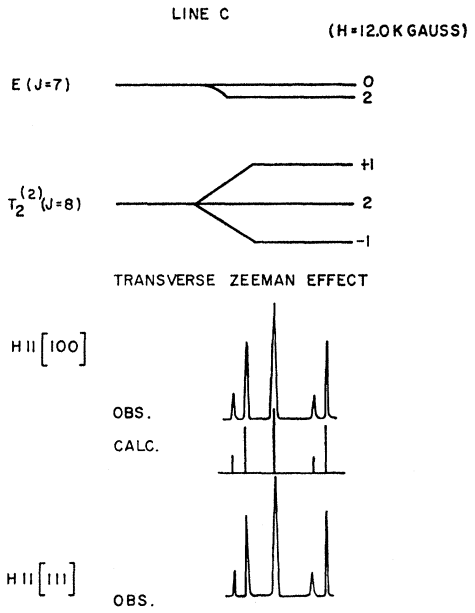

FIG. 4. Observed and calculated Zeeman pattern of the $|7E\rangle \rightarrow |8T_2^{(2)}\rangle$ transition (line C).

A. Since there are more than one independent observations on each state, the absolute shifts due to the nonlinear magnetic interactions of each sublevel can be evaluated.

Line D comes from the $|7E\rangle \rightarrow |8T_1^{(1)}\rangle$ transition (Fig. 5). From the study of this transition the behavior of the $|8T_1^{(1)}\rangle$ state can be determined. Line E and F, corresponding to the $|7T_2^{(2)}\rangle \rightarrow |8T_1^{(1)}\rangle$ and $|8E^{(2)}\rangle$ transitions, respectively (Figs. 6 and 7), gives the g value of the $|7T_2^{(2)}\rangle$ state. These last three lines can only be observed in fluorescence at liquid nitrogen temperature, and their intensities are somewhat weaker. While the signal to noise ratio was not sufficient for detailed study of the intensity pattern of the Zeeman components, it was sufficient to determine the g values. The data for the lines is summarized in Table I. The patterns observed are consistent with magnetic dipole patterns within the experimental accuracy, and the observed g values agree with the calculated ones using the wave function of Appendix I.[4]

IV. ORIENTATION DEPENDENCE OF THE ZEEMAN PATTERN OF THE LASER LINE

The $CaF_2:Dy^{2+}$ system was operated as an optical maser,[5] and as a laser it has a number of interesting characteristics. The fluorescent line width of the laser line (line A see Table II)[4] is narrower than the cavity mode separation for a 1-in. long crystal, and the laser operates in a single longitudinal mode. Zeeman tuning of the laser has been demonstrated previously.[6] The behavior of the laser in a magnetic field is not completely understood yet, and it was found that Zeeman tuning could only be achieved in certain oriented crystals.

Hence, it was desirable to analyze the orientation dependence of this transition in some detail.

The transition takes place between states $|7T_1^{(2)}\rangle$ and $|8T_2^{(2)}\rangle$. To calculate the magnetic dipole transition probabilities between the two states we need the matrix elements of the magnetic dipole operator

$$\mathfrak{y}=\sum_i \frac{e}{2m_ic}(\mathbf{l}_i+2\mathbf{s}_i),$$

which in the Russell Saunders approximation, reduces to $\mu \leftarrow = g\beta\mathbf{J}$. In the cubic group, the operator $\mathbf{J}$ transforms like T_1.

The relative intensities and polarizations of the Zeeman split components of the $|7T_1^{(2)}\rangle$ to $|8T_2^{(2)}\rangle$ transition can be calculated using only the symmetry properties of these states plus the realization that the magnetic dipole operator $\mathfrak{y}$ has T_1 symmetry. Or, what is simpler, one may use the property that the T_1 state transforms isomorphic to the $J=1$ orbital wave functions $|11\rangle$, $|10\rangle$, $|1-1\rangle$ and the T_2 state transforms isomorphic to the $J=2$ orbital wave functions $[|2-1\rangle$, $1\sqrt{2}(|22\rangle-|2-2\rangle)$, $-|21\rangle]$. Then, if the magnetic interaction $-\mathfrak{y}\cdot\mathbf{H}$ is put into the form

$$-g\beta H[-J_1\alpha_{-1}+J_0\alpha_0-J_{-1}\alpha_1], \tag{1}$$

where J_i and α_i are the irreducible tensor forms of the angular momentum and the unit vector in the magnetic field direction, respectively, the Hamiltonian for each of these two states becomes

$$H_{ij}(\gamma)=-g^\gamma\beta H\begin{pmatrix}\alpha_0 & -\alpha_1^* & 0\\ -\alpha_1 & 0 & -\alpha_1^*\\ 0 & -\alpha_1 & -\alpha_0\end{pmatrix}$$
$$\gamma=T_1 \text{ or } T_2,\quad i,j=1,0,-1 \text{ for } T_1,\quad \text{and}\quad -1,2,1 \text{ for } T_2, \tag{2}$$

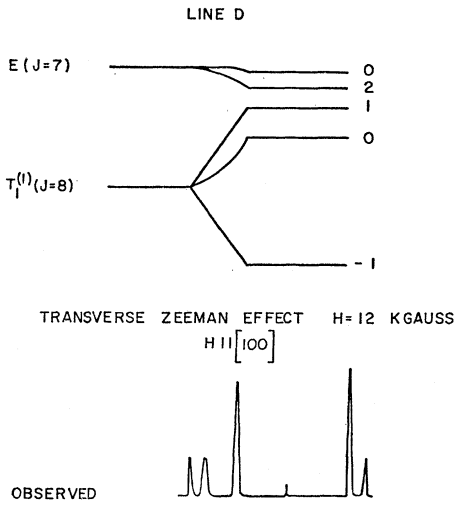

FIG. 5. Observed transverse Zeeman pattern of the $|7E\rangle \rightarrow |8T_1^{(1)}\rangle$ transition (line D).

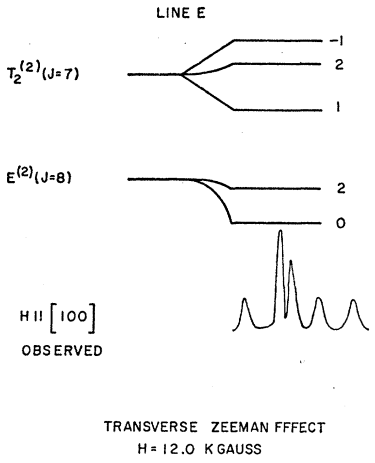

FIG. 6. Transverse Zeeman pattern of the $|7T_2^{(2)}\rangle \rightarrow |8E\rangle$ transition (line E).

where, if the direction of the magnetic field relative to the crystal axes [100], [010), and [001] is given in the usual polar coordinates, we have

$$\alpha_0=\cos\theta \quad \text{and} \quad \alpha_1=-(\sin\theta e^{i\psi})/\sqrt{2}. \tag{3}$$

Thus, the magnetic interaction is diagonal in this representation if the field lies along the [001] direction. The general Hamiltonian is diagonalized by the unitary transformation

$$U=\begin{pmatrix}\frac{1}{2}(1+\cos\theta)e^{i\psi} & \sin\theta/\sqrt{2} & \frac{1}{2}(1-\cos\theta)e^{-i\psi}\\ -(\sin\theta/\sqrt{2})e^{i\psi} & \cos\theta & (\sin\theta/\sqrt{2})e^{-i\psi}\\ \frac{1}{2}(1-\cos\theta)e^{i\psi} & -\sin\theta/\sqrt{2} & \frac{1}{2}(1+\cos\theta)e^{-i\psi}\end{pmatrix}, \tag{4}$$

to give

$$H_{ij}'=UHU^{-1}=-g^\gamma\beta|\mathbf{H}|\begin{pmatrix}1&0&0\\0&0&0\\0&0&-1\end{pmatrix}. \tag{5}$$

The fact that the states are split isotropically into three equally spaced levels is not surprising since the T_1 state is isomorphic to a $J=1$ state and so it acts like a free P state in a magnetic field. It is now convenient to retain the original labels for these magnetic sublevels in this new representation; hence the indices i, j take on the values 1, 0, -1 for the T_1 state and -1, 2, 1 for the T_2 state. We now need the matrix elements of the magnetic dipole operator between these states in order to be able to calculate the radiation patterns of the various transitions. In the original representation, we have

$$\langle T_{2i}|\mu_0|T_{1j}\rangle=\begin{pmatrix}0&0&1\\0&0&0\\-1&0&0\end{pmatrix}\langle T_2\|g\|T_1\rangle\beta \qquad \begin{matrix}i=-1,2,1,\\ j=1,0,-1,\end{matrix}$$

$$\langle T_{2i}|\mu_{+1}|T_{1j}\rangle=\langle\|g\|\rangle\beta\begin{pmatrix}0&0&0\\1&0&0\\0&-1&0\end{pmatrix},$$

and

$$\langle T_{2i}|\mu_{-1}|T_{1j}\rangle=\langle\|g\|\rangle\beta\begin{pmatrix}0&1&0\\0&0&-1\\0&0&0\end{pmatrix}=\mu_1{}^+, \tag{6}$$

which can be calculated in the diagonal representation by using the same unitary transformation U to give

$$\mu_0' = U\mu_0 U^{-1} = \langle\|g\|\rangle\beta$$

$$\times\begin{bmatrix} \frac{1}{2}i\sin^2\theta\sin2\psi & [(\sin\theta)/\sqrt{2}][\cos2\psi + i\cos\theta\sin2\psi] & \cos\theta\cos2\psi + \frac{1}{2}i[1+\cos^2\theta]\sin2\psi \\ [-\sin\theta/\sqrt{2}][\cos2\psi - i\cos\theta\sin2\psi] & -i\sin^2\theta\sin2\psi & [-\sin\theta/\sqrt{2}][\cos2\psi + i\cos\theta\sin2\psi] \\ -\cos\theta\cos2\psi + \frac{1}{2}i[1+\cos^2\theta]\sin2\psi & [(\sin\theta)/\sqrt{2}][\cos2\psi - i\cos\theta\sin2\psi] & \frac{1}{2}i\sin^2\theta\sin2\psi \end{bmatrix},$$

and

$$\mu_1' = U\mu_1 U^{-1} = \langle\|g\|\rangle\beta e^{-i\psi}\begin{bmatrix} (\sin2\theta)/2\sqrt{2} & \frac{1}{2}[2\cos^2\theta - 1 - \cos\theta] & [\sin\theta/\sqrt{2}][1-\cos\theta] \\ \frac{1}{2}[2\cos^2\theta - 1 + \cos\theta] & (-\sin2\theta)/\sqrt{2} & -\frac{1}{2}[2\cos^2\theta - 1 - \cos\theta] \\ (-\sin\theta[1+\cos\theta])/\sqrt{2} & -\frac{1}{2}[2\cos^2\theta - 1 + \cos\theta] & (\sin2\theta)/2\sqrt{2} \end{bmatrix}. \quad (7)$$

Example 1. Consider the case where the magnetic field lies in the [001] direction. Then the matrix elements of the magnetic dipole operator are given by (6) and we have (a) all $\Delta m = \pm 2$ transitions are not allowed. (b) $\Delta m = +1$ transitions are right circularly polarized along the field and $\Delta m = -1$ are left circularly polarized. (c) $\Delta m = 0$ transitions are linearly polarized with their magnetic vector along the field direction.

Example 2. Consider the case where the field direction lies in the [111] direction; then the most convenient components of the magnetic dipole operator are

$$\mu_1 = 1/\sqrt{2}[\mu_x - \mu_y],$$
$$\mu_2 = 1/\sqrt{6}[\mu_x + \mu_y - 2\mu_z],$$
$$\mu_3 = 1/\sqrt{3}[\mu_x + \mu_y + \mu_z],$$

and the circular polarization forms $\mu_+ = [\mu_2 + i\mu_1]/\sqrt{2}$ and $\mu_- = [\mu_2 - i\mu_1]/\sqrt{2}$. These can be calculated from (7) to give

$$\mu_3 = i\langle g\rangle\beta/\sqrt{3}\begin{bmatrix} 1 & 0 & 0 \\ 0 & -2 & 0 \\ 0 & 0 & 1 \end{bmatrix}; \quad \mu_+ = \langle g\rangle\beta/\sqrt{3}\begin{bmatrix} 0 & 1 & 0 \\ 0 & 0 & -1 \\ 2 & 0 & 0 \end{bmatrix};$$

and

$$\mu_- = \langle g\rangle\beta/\sqrt{3}\begin{bmatrix} 0 & 0 & 2 \\ 1 & 0 & 0 \\ 0 & -1 & 0 \end{bmatrix}.$$

These give the results that the $\Delta m = 2$ transitions are linearly polarized with their magnetic vector along the field direction and all the other transitions are right or left circularly polarized along the field. The relative intensities for these two cases are summarized in Fig. 2.

A few general observations can be made about this problem. First of all only in the above two cases is the intensity distribution isotropic in the plane perpendicular to the magnetic field. This is because these are the only two axes with higher than twofold symmetry. Secondly, if one makes frequency measurements along a crystal field axis with no polarization selection in the intensity pattern is given by

$$|\langle T_{1i}|\mu_1|T_{2j}\rangle|^2 + |\langle T_{1i}|\mu_{-1}|T_{2j}\rangle|^2.$$

But the only dependence μ_1 and μ_{-1} have on the azimuthal angle ψ is through the multiplicative factor $e^{\pm i\psi}$ which vanishes in the above expressions. Hence, the intensity distribution as measured in this way depends only on the angle between the field and the crystalline axis along which the observations are made and is independent of the orientation of the other two axes. Thirdly, only the $\Delta m = 0$ transitions have a simple expression for a general field direction, namely these transitions are always linearly polarized with their magnetic field vectors in the direction $\mathbf{p} = \alpha_y\alpha_z\mathbf{e}_x + \alpha_x\alpha_z\mathbf{e}_y + \alpha_x\alpha_y\mathbf{e}_z$, where α_x, α_y, and α_z are the direction cosines of the magnetic field from the three crystalline axes. It can be easily verified that this transition probability reaches a maximum for the field in the [111] direction and vanishes along the cubic axes.

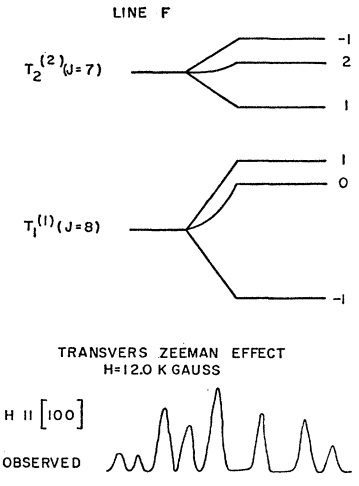

FIG. 7. Transverse Zeeman pattern of the $|7T_2^{(2)}\rangle \rightarrow |8T_1^{(1)}\rangle$ transition (line F).

V. MAGNETIC INTERACTION AMONG THE LOWEST CRYSTALLINE STARK LEVELS

The three crystalline Stark levels of the ground state are separated by small energies as shown on Fig. 1 and the magnetic interaction among these three states is appreciable. The shifts of the Zeeman components of these levels are shown in Fig. 8, for the case of H along a [100] axis. The strongest interaction is among the two lowest levels, the $|8T_1^{(1)}\rangle$ and $|8E^{(2)}\rangle$, which are separated by 4.9 cm^{-1}. To solve the interaction for the eight Zeeman sublevels for an arbitrary orientation is complex and requires the diagonalization of an 8×8 matrix. However, for the experimental situation of Fig. 8, ($H\|[100]$), the matrix can be reduced to four 2×2

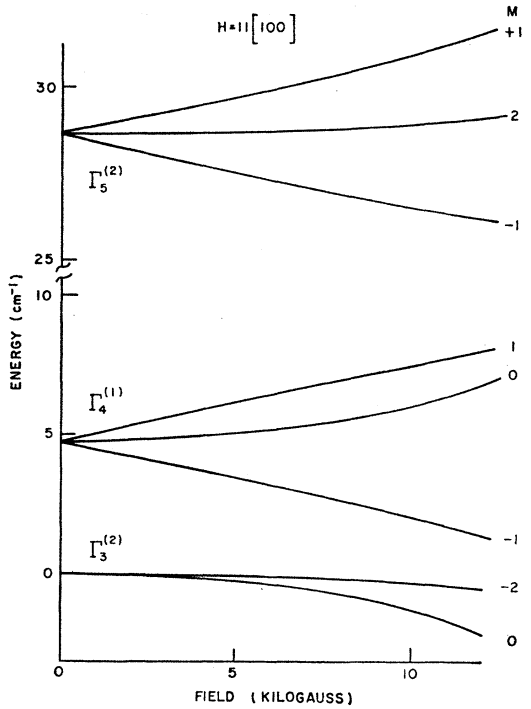

FIG. 8. The nonlinear splitting pattern of the three lowest levels of the $^5I_8$ ground state as a function of magnetic field $H\|[100]$.

matrices, and the absolute value of the coefficient of the quadratic splitting factor can be calculated by second-order perturbation theory. The energy shift, for example, for the $|8E^{(2)}0\rangle$ component due to the magnetic mixing with the $|8T_1^{(1)}0\rangle$ component for $H\|[100]$ will be

$$\delta E=(g\beta H)^2\frac{|\langle 8E^{(2)}0|J_z|8T_1^{(1)}0\rangle|^2}{\Delta},$$

where δE is in cm^{-1}, $g=\frac{5}{4}$ is the Lande factor, $\Delta=E|8T^1\rangle-E|8E^2\rangle=4.9$ cm^{-1}. If H is kG, $\beta=0.0467$ cm^{-1}/kG.

Similar matrix elements were evaluated for all the observed levels, using only second order perturbation, and mixing only with next-nearest-neighbor levels. The agreement between the calculated and observed values is good.

In the above approximation, when the field is along [100] the ground $|8E^{(2)}\rangle$ state will be split by the nonlinear interaction; however, paramagnetic resonance is not observable between the $\mu=0$ and $\mu=2$ sublevels. For any other orientation of H_1, the nonlinear interaction will admix $\mu=\pm1$ character into both sublevels, and resonance is observed.[8] At sufficiently high fields, resonance between the $|8E^{(2)}0\rangle$ and $|8T_1^{(1)}1\rangle$ Zeeman levels should also be observable.

VI. CONCLUSIONS

In conclusion, we can state that $^5I_7$–$^5I_8$ transitions in the CaF_2:Dy^{2+} system are of magnetic dipole origin. This result is not surprising; the cubic symmetry of the static crystal field does not admix configurations, and the $4f$–$4f$ electric dipole transitions remain strictly forbidden. The allowed electric quadrupole transitions were estimated to be about 100 times weaker than the magnetic dipole transitions. An upper limit of this estimation was confirmed in the case of the $|7T_1^{(2)}\rightarrow|8T_1^1\rangle$ transition, where the magnetic dipole transition is not observed. Electric quadrupole transition is allowed, and the signal-to-noise ratio of the other magnetic dipole transitions was good enough to see a line 500 times weaker. Electric dipole transitions induced by the dynamic crystal field do occur (see Ref. 4), but they always involve a change in the vibrational quantum number and cannot contribute to the intensity of the unshifted transition between the crystal field levels.

From the study of the g values and the Zeeman patterns, the symmetries of six levels were determined. The ratio of the B_6/B_4 parameter quoted in Ref. 4, $B_6/B_4=-0.268$, was confirmed by the good agreement between the calculated and observed g values. The orientation dependence of the Zeeman pattern of the $|7T_1^{(2)}\rangle\rightarrow|8T_2^{(2)}\rangle$ transition was analyzed and the observed variation of the pattern could be well accounted for assuming magnetic dipole transition. Effects of the magnetic interactions among Stark levels were observed and explained and the paramagnetic behavior of the ground state[8] was predicted.

ACKNOWLEDGMENTS

The authors wish to acknowledge many helpful discussions with H. R. Lewis, S. R. Polo, E. S. Sabisky, and H. A. Weakliem. The experimental assistance of D. L. Kupper is appreciated.

[8] E. S. Sabisky, J. Chem. Phys. (to be published).